International Journal of
Science and Engineering Investigations vol. 9, issue 101, June 2020
Received on June 17, 2020 ISSN: 2251-8843

Fabrication of Carbon Nanotube (CNT) by Chemical Vapor Deposition and Investigate the Second Harmonic Response from CNT/Peptide and Si/SiO_2/Peptide Interfaces

Munaly Akter[1], Md. Masud Parvez[2], Md. Ehasanul Haque[3], Humayra Ferdous[4], Md. Abdul Matin[5]
[1,5]Department of Materials Science and Engineering, Rajshahi University, Motihar, Rajshahi-6300, Bangladesh
[2,3,4]Department of Physics, American International University-Bangladesh (AIUB), Kuril, Dhaka-1229, Bangladesh
([1]akter_munaly88@yahoo.com, [2]masud.parvez@aiub.edu, [3]ehasanul@aiub.edu, [4]hferdous@aiub.edu, [5]matinmst@ru.ac.bd)

Abstract-We observed the second harmonic generation (SHG) intensity from the peptide molecules absorbed carbon nanotube surface grown on the Si/SiO_2/Co substrate. We dropped different concentrations of peptide molecules such as 100nM, 1μM and 10μM on the three Si/SiO_2/Co/CNT substrate individually. The SHG intensity was measured from the CNT/PEP interface by using 1.17 eV pulsed laser light. The results show that, the SHG intensity increased with increasing the peptide concentrations. In order to confirm about the SHG signal detected from the CNT/PEP interface, we dropped similar concentrations of peptide molecule on the three different Si/SiO_2 substrate having no CNT layer individually and we observed the same results as found for CNT/PEP interface. In this case, the SHG intensity also increased with increasing the concentrations of peptide molecules on the surface. So, the generation of second harmonic signal is due the peptide molecule for both cases.

Keywords- *Carbon Nanotubes, Peptide Molecules, Second Harmonic Generation, Pulsed Laser*

I. INTRODUCTION

Carbon nanotubes (CNTs) have been recognized originally by Sumio lijima in 1991 [1]. Graphene sheets are rolled up to prepare CNTs. CNTs have large variety of physical properties due to having different individual graphene layer. Due to having wide variety of mechanical strengths as well as electronic structures and outstanding optical properties CNTs can show potential electrical and optical applications [2]. Due to having many interesting features and applications in the field of electronics and optics, it needs quality characterization methods that are specific and cost-effective to determine the nonlinear optical property.

Now-a-days nonlinear techniques interestingly used extensively due to the probability of gaining remarkably large nonlinear optical responses from nanomaterials that can provide complementary information [3]. Second harmonic generation (SHG) is very promising nonlinear technique to explore electronic information from the nanomaterials. SHG methods are known to symmetry sensitive method and are not forbidden in noncentrosymmetric materials with in the electric-dipole approximation due to the interaction between light and matter [4]. However, SHG signals are not obtainable from centrosymmetric media [4]. When the incident light of frequency ω comes to the asymmetry medium, the light of frequency 2ω will be generated. This phenomenon is SHG. In addition, when incident light of frequency ω comes to the symmetry medium, the light of frequency 2 ω will not be generated in electric dipole approximation. Therefore, SHG spectroscopy is sensitive to surface and interface where the spatial symmetry is broken. In case of our growing CNT, it is randomly grown on the substrate and the peptide molecules are also randomly distributed as irregular film on the CNT surface. So, the surface is noncentrosymmetric and can generate SHG.

Okawara et al. investigated the CNT film surface grown on SiO_2 substrate by SHG technique. They used 1064 nm wavelength of laser light as fundamental radiation and observed the alignment of the grown CNT film after analyzing the SHG signal [5]. Some other researchers found that the SHG signal generated from CNT due to having local imperfections, deformation, chirality that resulted from nonracemic assembly at the internal structure of CNT [6-9]. L. De Dominicis et al. investigated single-walled carbon nanotube surface by SHG technique and found that the main source of SHG generation is the structural defects or chirality [10,11]. S. Fujii et al. observed the SHG signal from the monolayers of cyclic peptides which is self-assembled [12]. Nakayama et al. observed the SHG signal from helical peptides attached with chromophore to evaluate self-assembled monolayer structure of a stereocomplex of helical peptides [13]. The SHG signal was observed from the different types of peptides and polypeptides that carries polarizable groups. The strongest SHG signal was found from monopeptide and dipeptide derivatives of p-nitrophenylalanine [14].

Above literature reveals that many researchers have been investigated individually either CNT or peptide surface by SHG technique. However, very limited study could be found on CNT/Peptide interface by SHG method. So, we intended to check the SHG responses from samples with or without CNT

containing same concentrations of peptide molecules to confirm the role of CNT and how the SHG responses could be changed with different concentrations of peptides dropped on CNT. The main purposes of our work were to measure SHG intensity for checking the immobilization of peptide molecules on CNT surface and make a significant improvement of bio-sensing materials field. As the SHG method is new to apply for investigating the peptide molecules, it is our great interest to observe the SHG response from CNT/PEP interface

In this work, we synthesized the CNTs on to the $Si/SiO_2/Co$ substrate by chemical vapor deposition (CVD) method. After that, we dropped different concentrations such as 100nM, 1μM and 10μM of peptide molecules on the three individual $Si/SiO_2/Co/CNTs$ substrate's surface by using pipettes to fabricate peptide aptamer. We also have fabricated peptide aptamer on the surface of Si/SiO_2 substrate in a similar way to confirm the effect of SHG signal on the variant concentrations of peptide molecules. Interestingly we found that, the SHG intensity was increased with increasing the concentration of peptide molecules for both types of substrate.

II. MATERIALS AND METHODS

A. Synthesis of carbon nanotube (CNT) using ethanol chemical vapor deposition (CVD) method

In this work, CNT was fabricated by CVD technique. Figure 1 exhibits the schematic diagram of CVD system. In order to fabricate CNT, the source of carbon was needed undoubtedly, and ethanol was used as carbon source. A temperature controller has been used to control the temperature of the system. During ethanol supply, Argon gas was introduced through mass-flow controller into the chamber for keeping the system stable. Vacuum was made inside the chamber by using a rotary pump. A manometer was set to observe the pressure of the chamber.

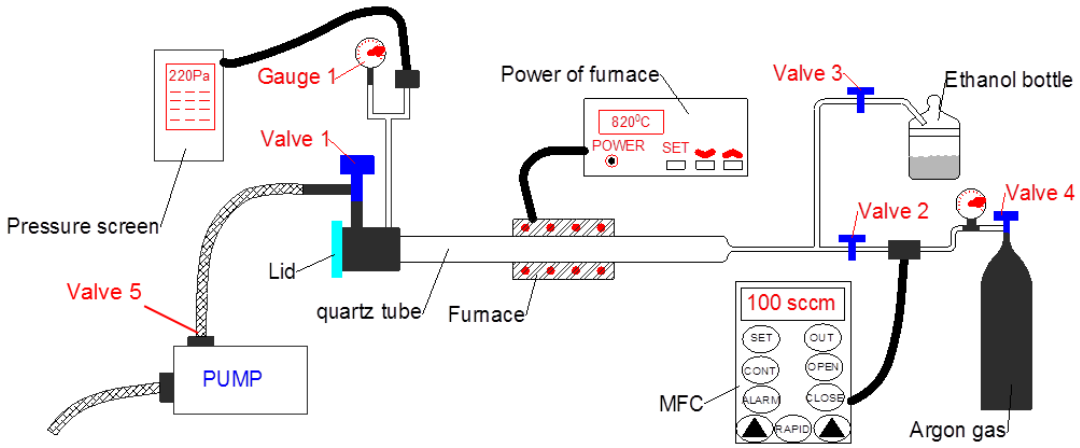

Figure 1. Schematic diagram for CNT synthesis by CVD technique

Fig. 2 and 3 exhibit the fabrication process of $Si/SiO_2/Co/CNT/PEP$ and $Si/SiO_2/PEP$ sample respectively. In case of fabrication of $Si/SiO_2/Co/CNT/PEP$ sample, a commercial SiO_2 (100nm)/p^+-Si substrate was cleaned with piranha solution. Then, we deposited 5-nm-thick Co film onto the substrate as a catalyst by using e-beam evaporator MUE-ECO-EB (ALVAC) at 0.01 nm/s deposition rate. Substrate containing Co catalyst thin film was set inside the CVD chamber for CNT growth. In order to remove the residual gases from the chamber made up of quartz tube, 10 Pa pressure and 800°C temperature were maintained during evacuation process. The sample was introduced inside the chamber after the chamber was being cooled at room temperature.

For having optimum condition, the chamber was started evacuating at increasing temperature. After reaching temperature of 820°C, Ar gas (100 sccm) was inserted in a controlled manner by using mass flow controller only for 10 minutes to achieve the thermal equilibrium state of the entire system. To maintain the desired pressure (220 Pa) ethanol was then inserted into the chamber for 30 min. The chamber was then allowed to cool down to room temperature naturally for collecting the sample after the completion of CNT growth.

After that we dropped the peptide molecules with a variant concentration (100 nM, 1 μM, and 10 μM) using pipettes on to the three individual $Si/SiO_2/Co/CNT$ and similarly Si/SiO_2 samples. Then we dried the samples for 1 day at room temperature.

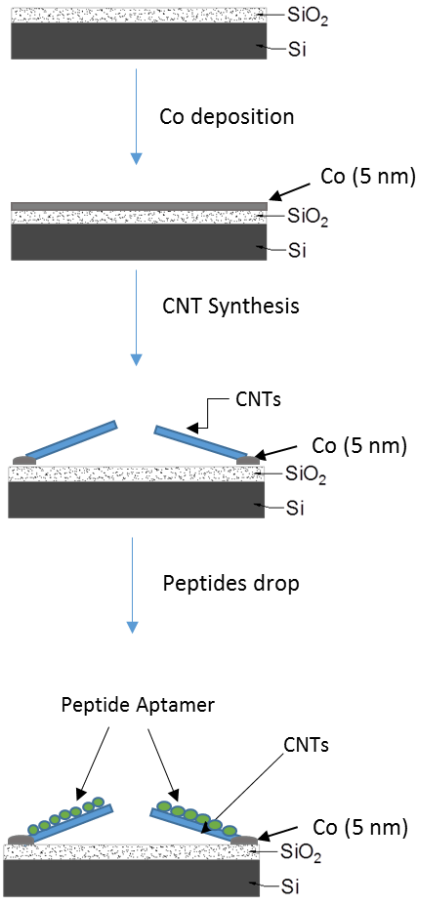

Figure 2. The procedure of CNT synthesis and fabrication of peptide aptamer

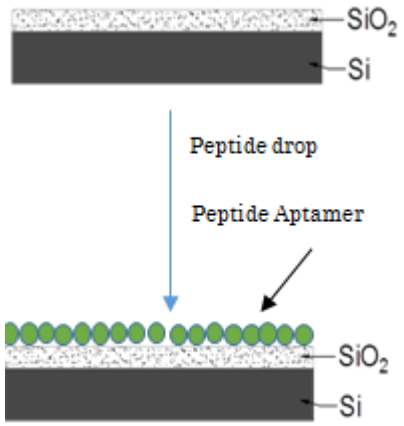

Figure 3. Fabrication of peptide aptamer on Si/SiO_2 substrate

B. *Peptide Aptamer*

Pierre Colas et al. discovered peptide aptamers in 1996 [15]. Peptide aptamers are small artificial recognition proteins that consist a variable peptide sequence with affinity for a given target protein. This variable peptide sequence is able to prepare "scaffold" known as very stable backbone of protein [16-21]. Peptide aptamers can be produced and selected *in vivo* from combinatorial libraries based on their affinity to the target protein and expressed in bacterial cells such as E. coli. Both termini of the variable peptide sequence are embedded ("double constrained") within an inert and constant scaffold protein. This double constraint distinguishes peptide aptamer from other classes of constrained combinatorial proteins (such as antibodies, antibody fragments and other non-antibody scaffold-based molecules) which consist of random peptide sequences embedded to a carrier protein [22] (Fig. 4). These molecules are recognized as more complex compared to the peptide aptamers as the target-binding surfaces consist of noncontiguous peptides sequences disseminated on several secondary structural elements or across several variable loops. Moreover, the disulfide bonds are created by these molecules play an important role to fold properly and are thus ill suited to target intracellular proteins [16].

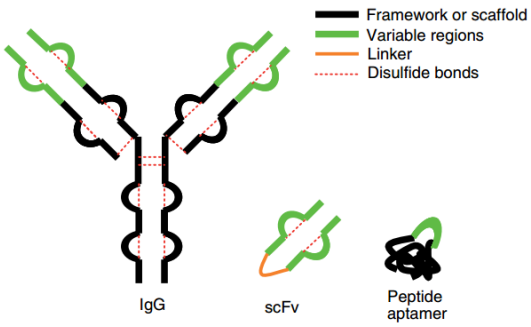

Figure 4. Comparison among different types of constrained combinatorial recognition proteins. IgG, immunoglobulin G, single-chain Fv, antibody fragment [18].

Based on above mentioned reasons peptide aptamer is the promising candidate for many applications such as biosensor, CNT-FET etc. In this work, we offer SHG method to check the immobilization of peptide aptamer on to the $Si/SiO_2/Co/CNT$ substrate.

C. *SHG Intensity Measurement*

A mode-locked Nd^{3+}:YAG picosecond laser was used to detect SHG signal from the sample surface. Pulse width and repetition rate were 30 ps and 10 Hz respectively, recorded at the output of the excitation source. The sample was kept on to the automatic rotation stage to measure the SHG signal. The incident light having photon energy of 1.17 eV was illuminated on the samples at an angle of 45° after passing through a prism, mirrir, half-wave plate, polarizer, 2ω cut filter and a lens in different experiment for individual samples. To avoid damaging the sample, the average energy of the incident beam was maintained approximately 50 μJ/pulse. The reflected radiation (including SHG signal) was passed through a presettled lens, ω cut filter, output polarizer, depolarizer, lens, monochromator and finally by a photomultiplier tube. After that we collected the data as the SHG intensity processed in PC.

III. RESULTS AND DISCUSSION

A. SHG intensity of bare CNTs and variant concentration of CNTs/PEP

We measured the SHG intensity of bare CNTs, CNTs/PEP (100nM), CNTs/PEP (1μM) and CNTs/PEP (10μM). The last three sample we prepared by the process of peptide aptamer. We dropped the peptide molecules by using pipettes on the CNTs samples. Figure 5, 6, 7 and 8 showing the SHG intensity of bare CNTs, CNTs/PEP (100nM), CNTs/PEP (1μM) and CNTs/PEP (10μM) respectively. The horizontal axis is the wavelength of monochromator and the vertical axis is the SHG intensity from the above-mentioned samples. We changed the monochromator wavelength manually and measured the SHG intensity for each sample. We observed that, the highest SHG intensity was recorded at wavelength 532 nm. When we increase or decrease manually the wavelength of monochromator from 532 nm incrementally, the SHG intensity also decreased in most cases. This observation proves that, the recorded signal is SHG signal because for 1064 nm fundamental laser probe, the highest SHG intensity peak should be recorded at 532 nm wavelength. In our experimental case, we also observed the highest SHG intensity peak due to the resonance occurred at wavelength 532 nm. We have fitted (Gaussian) our experimental data by using MATLAB software.

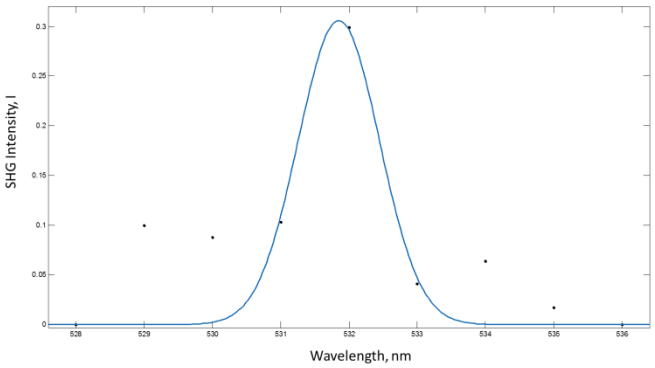

Figure 5. SHG intensity of bare CNTs in terms of wavelength

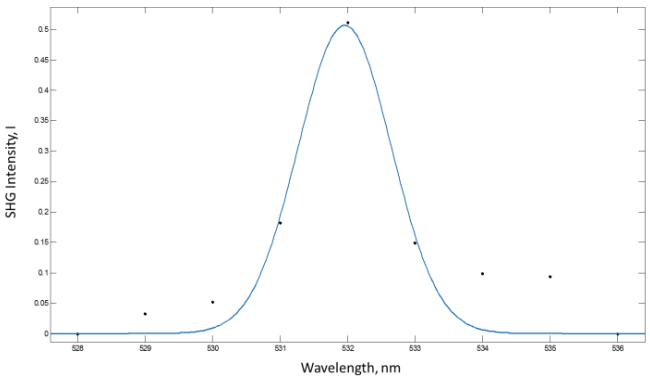

Figure 6. SHG intensity of CNTs with 100 nM peptide in terms of wavelength

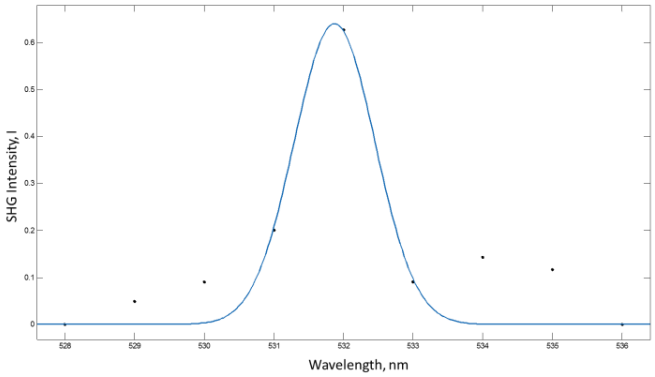

Figure 7. SHG intensity of CNTs with 1 μM peptide in terms of wavelength

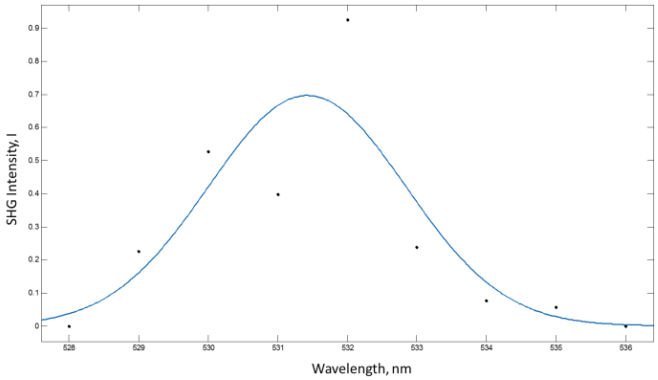

Figure 8. SHG intensity of CNTs along with 10 μM peptide in terms of wavelength

Fig. 9 shows the SHG intensity of bare CNTs and CNTs with variant concentration of peptide molecules. From the figure, the SHG intensity increased with increasing the concentration of peptide molecules on the CNTs. We assumed highest values of SHG intensity, and it was observed at the wavelength of 532 nm. This highest SHG intensity value obtained from Fig. 5, 6, 7 and 8. As we introduced the incident beam of wavelength 1064 nm, so, it is obvious to obtain significant SHG signal at the wavelength of 532 nm.

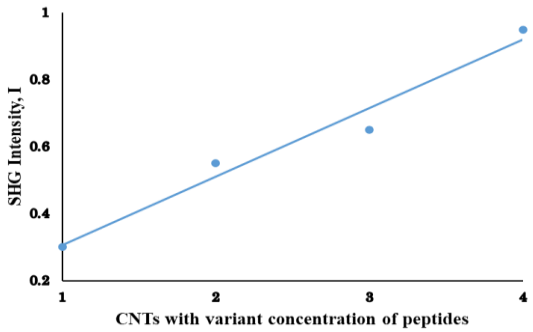

Figure 9. SHG intensity from CNTs with variant concentration of peptides at wavelength of 532 nm. In X-axis: **1, 2, 3 & 4** correspond to CNTs without peptides, CNTs with 100 nM peptides, CNTs with 1 μM peptides, CNTs with 10 μM peptides respectively.

B. SHG intensity from bare Si/SiO_2 and Si/SiO_2 with variant concentration of peptide molecules

We measured the SHG intensity of bare Si/SiO_2 and Si/SiO_2 along with variant concentration (100 nM, 1µM and 10 µM) of peptide molecules. We prepared these samples by the process of peptide aptamer. We dropped the peptide molecules by using pipettes individually on the three Si/SiO_2 substrates with concentrations 100nM, 1µM and 10 µM respectively. Figure 10, 11, 12 and 13 showing the SHG intensity of bare Si/SiO_2, Si/SiO_2/PEP (100 nM), Si/SiO_2/PEP (1 µM) and Si/SiO_2/PEP (10 µM) respectively. The horizontal axis is the wavelength of monochromator and the vertical axis is the SHG intensity from the above-mentioned samples. We changed the monochromator wavelength and measured the SHG intensity for each sample. We observed that, the highest SHG intensity was recorded at wavelength 532 nm. When we increased or decreased manually the wavelength of monochromator from 532 nm incrementally, the SHG intensity also decreased in most cases. This observation proves that, the recorded signal is SHG signal because for 1064 nm fundamental laser probe, the highest SHG intensity peak should be recorded at 532 nm wavelength. In our experimental case, we also observed the highest SHG intensity peak due to the resonance occurred at wavelength 532 nm. We have fitted (Gaussian) our experimental data by using MATLAB software.

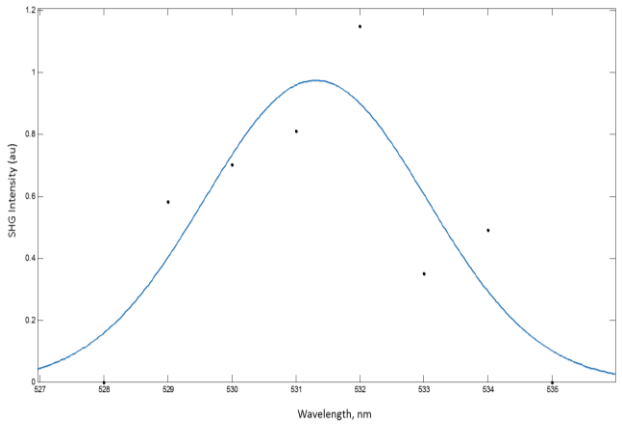

Figure 10. SHG intensity of bare Si/SiO_2 as a function of wavelength.

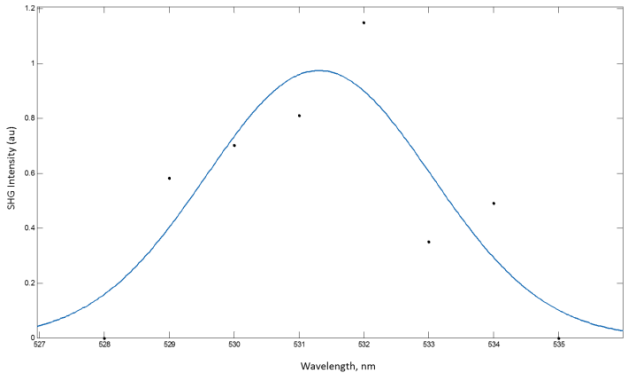

Figure 11. SHG intensity of Si/SiO_2 with 100 nM peptides as a function of wavelength.

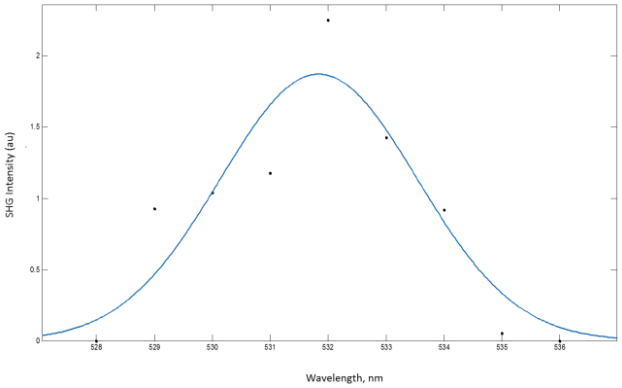

Figure 12. SHG intensity of Si/SiO_2 with 1 µM peptides as a function of wavelength.

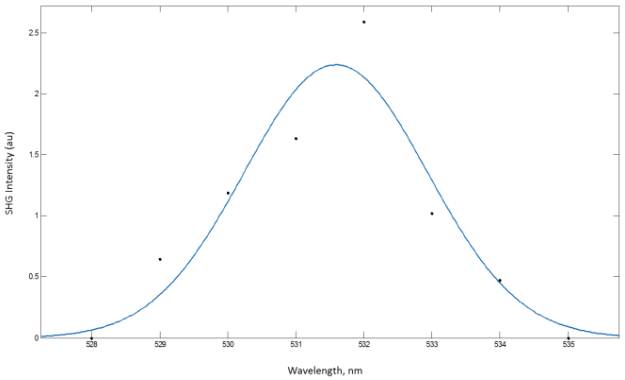

Figure 13. SHG intensity of Si/SiO_2 along with 10 µM peptides as a function of wavelength.

Figure 14 shows that, the SHG intensity of bare Si/SiO_2 and Si/SiO_2 along with variant concentration (100 nM, 1µM and 10 µM) of peptide molecules. From the Fig. 14, SHG intensity increased with increasing the concentration of peptide molecules on the Si/SiO_2 substrate. We assumed highest values of SHG intensity, and it was observed at the wavelength of 532 nm. This highest SHG intensity value obtained from Fig. 10, 11, 12 and 13. As we introduced the incident beam of wavelength 1064 nm, So, it is obvious to obtain significant SHG signal at the wavelength of 532 nm.

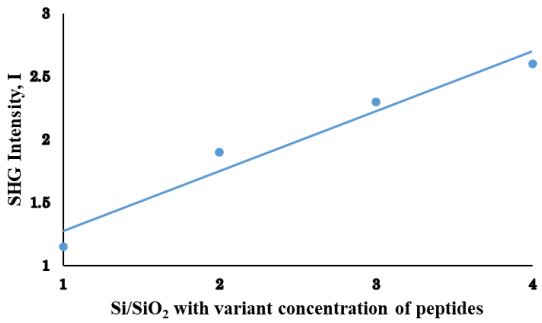

Figure 14. SHG intensity from Si/SiO_2 with variant concentrations of peptides at wavelength of 532 nm. In X-axis: **1, 2, 3 & 4** correspond to Si/SiO_2 without peptides, Si/SiO_2 with 100 nM peptides, Si/SiO_2 with 1 µM peptides, Si/SiO_2 with 10 µM peptides respectively.

C. SEM analysis

We also conducted the SEM analysis to confirm the fabrication of CNTs. Fig. 15 shows that, the CNTs grow on $Si/SiO_2/Co$ substrate. It seemed that, lots of amorphous carbon was existed on the $Si/SiO_2/Co/CNTs$ surface according to SEM image. These huge amounts of amorphous carbons are possible candidate for the generation of low SHG intensity. The magnification of the SEM image was 2μm.

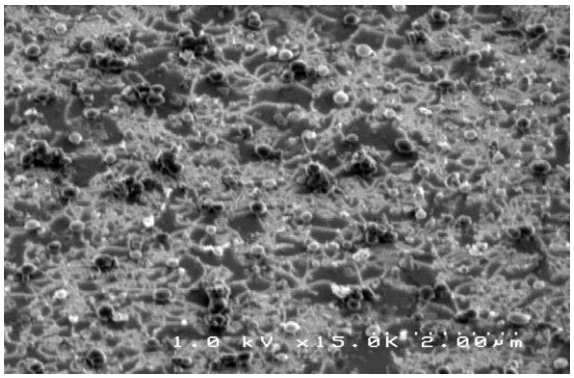

Figure 15. SEM image of CNTs fabricated on $Si/SiO_2/Co$ substrate.

D. Discussion

Peptide molecules have very large C-C chain structure and contains many kinds of bonding such as C-C, C-H, O-H, N-H, C-O etc. So as the concentration of peptide molecules are increased the number of these bonds are also increased. These bonds may create chirality. So, Probably, these bonds are responsible for increasing dipoles at the interface region causes strong SHG signal. The interaction between the electric field of incident laser light and the dipoles of the peptide molecule also increased as the concentrations of peptides on CNT or Si/SiO_2 surface increased gradually in each sample. So, the SHG intensity enhanced. Similarly, the SHG intensity increased with increasing the peptide concentration on the Si/SiO_2 substrate. The reason may be same.

The SHG intensity of bare Si/SiO_2 and Si/SiO_2 along with variant concentrations (100 nM, 1 μM and 10 μM) of peptide molecules are little greater than the SHG intensity of bare CNTs and CNTs with variant concentration (100 nM, 1 μM and 10 μM) of peptide molecules. The SHG intensity from CNT/PEP interface was observed but due to having some amorphous carbon on the surface of CNT, the SHG intensity is little lower compared to the SHG intensity observed from SiO_2/PEP interface although the chiral structure may exist. Si/SiO_2 shows semiconducting behavior as well. So, from the interface of Si/SiO_2/PEP, a little stronger SHG signal was detected compared to the interface of CNT/PEP.

IV. CONCLUSIONS

In this study, the CNT was fabricated on the $Si/SiO_2/Co$ substrate by chemical vapor deposition (CVD) method. Then we dropped variant concentrations peptide molecules on the CNT surface to from peptide aptamers and measured the SHG intensity from the CNT/PEP interface. As the peptide concentration increased the SHG intensity was also increased. In order to confirm the effect of peptide molecules, we also prepared the Si/SiO_2 substrate having no CNT layer and similarly dropped variant concentrations of peptide molecules on Si/SiO_2 substrate surface and measured the SHG intensity. In this case, the SHG intensity was also increased with increasing the peptide concentration just like previous case. So, the peptide molecules can generate SHG due to having different kinds of chemical bond. These chemical bonds may create chirality that may responsible for generating SHG signal. In this research, measurement of SHG intensity as a function of increasing concentrations of peptide molecules was our physical interest only.

REFERENCES

[1] **S.** lijima, "Helical micortubes of graphitic carbon, Nature," vol. 354, pp. 56-58, 1991.

[2] P. Avouris, Z. H. Chen & V. Perebeinos, "Carbon-based electronics," Nature Nanotechnology, vol. 2 no. 10, pp. 605-615, 2007.

[3] M. C. Hersam, "Progress towards monodisperse single-walled carbon nanotubes," Nature Nanotech., vol. 3, pp. 387-394, 2008.

[4] Y. R. Shen, "Surface properties probed by second-harmonic and sum-frequency generation," Nature, vol. 337, pp. 519-525, 1989.

[5] S. Okawara, M. Kudo, M. Miyamori, S. Ohno, Y. Shimazu, M. Tanaka & T. Suzuki, "Second-harmonic generation from supported carbon nanotube films grown by chemical vapor deposition on fused silica," Japanese Journal of Applied Physics, vol. 58, p. 032006, 2019.

[6] H. M. Su, J. T. Ye & K. S. Wong, "Resonant second-harmonic generation in monosized and aligned single-walled carbon nanotubes," Phys. Rev. B, vol. 77, p. 125428, 2008.

[7] S. O. Konorov, D. A. Akimov, A. A. Ivanov, M. V. Alfimov, S. Botti, R. Ciardi, L. D. Deominicis, L. Asilyan, A. A. Podshivalov, D. A. Sidorov-Biryukov, R. Fantoni & A. M. Zheltikov, "Femtosecond optical harmonic generation as a non-linear spectroscopic probe for carbon nanotubes," J. Raman Spectroscopy, vol. 34, pp. 1018-1024, 2003.

[8] D. A. Akimov, M. V. Alfimov, S. O. Konorov, A. A. Ivanov, S. Botti, A. A. Podshivalov, R. Ciardi, L. D. Deominicis, L. Asilyan, R. Fantoni & A. M. Zheltikov, "Generation of the second and third harmonics of femtosecond Cr: Forsterite-laser pulses by single-wall carbon nanotubes," Laser Physics, vol. 13, no. 10, pp. 1279-1283, 2003.

[9] S. Botti, R. Ciardi, L. D. Dominicis, L. Asilyan, R. Fantoni & T. Marolo, "DFWM measurements of third-order susceptibility of single-wall carbon nanotubes grown without catalyst," Chemical Physics Letter, vol. 378, pp. 117-121, 2003.

[10] L. D. Dominicis, S. Botti, L. S. Asilyan, R. Ciardi, R. Fantoni, M. L. Terranova, A. Fiori, S. Orlanducci, & R. Appolloni, "Second-and third-harmonic generation in single-walled carbon nanotubes at nanosecond time scale," Applied Physics. Letters, vol. 85, pp. 1418-1420, 2004.

[11] L. D. Dominicis, R. Fantoni, S. Botti, R. Ciardi, L. Asilyan, A. Fiori & S. Orlanducci, "Analysis of the chiral composition of a carbon nanotube surface by means of second harmonic generation," J. Raman Spectroscopy, vol. 36, pp. 165-170, 2005.

[12] S. Fujii, T. Morita, J. Umemura & S. Kimura, "Cyclic peptides as scaffold for oriented functional groups on surface," Thin Solid Films, vol. 503, pp. 224-229, 2006.

[13] H. Nakayama, T. Manaka, M. Iwamoto & S. Kimura, "Vertical orientation with a narrow distribution of helical peptides immobilized on a quartz substrate by stereocomplex formation," Soft Matter, vol. 8**,** pp. 3387–3392, 2012.

[14] S. Tokutake, Y. Imanishi & M. Sisido, "Efficiency of Second Harmonic Generation from Amino Acids, Peptides, and Polypeptides Carrying

Polarizable Aromatic Groups," Mol. Cryst. Liq. Cryst., vol. 170, pp. 245-257, 1989.

[15] P. Colas, B. Cohen, T. Jessen, I. Grishina, J. McCoy & R. Brent, "Genetic selection of peptide aptamers that recognize and inhibit cyclin-dependent kinase 2," Nature, vol. 380, pp. 548-550, 1996.

[16] I. C. Baines & P. Colas, "Peptide aptamers as guides for small-molecule drug discovery," Drug Discovery Today, vol. 11, no. 7–8, pp. 334-341, 2006.

[17] F. Hoppe-Seyler & K. Butz, "Peptide aptamers: powerful new tools for molecular medicine," Journal of Molecular Medicine, vol. 78, pp. 426-430, 2000.

[18] P. Colas, "The eleven-year switch of peptide aptamers," Journal of Biology, vol. 7, no. 2, pp. 1-5, 2008.

[19] F. Hoppe-Seyler, C. Mertens, C. Denk, B. A. Fitscher, B. Klevenz, E. Tomai & K. Butz, "Peptide aptamers: new tools to study protein interactions," The Journal of Steroid Biochemistry and Molecular Biology, vol. 78, no. 2, pp. 105-111, 2001.

[20] M. Crawford, R. Woodman & P. K. Ferrigno, "Peptide aptamers: Tools for biology and drug discovery," Briefings in Functional Genomics and Proteomics, vol. 2, no. 1, pp. 72-79, 2003.

[21] F. Hoppe-Seyler, I. Crnkovic-Mertens, E. Tomai & K. Butz, "Peptide Aptamers: Specific Inhibitors of Protein Function," Current Molecular Medicine, vol. 4, no. 5, pp. 529-538, 2004.

[22] M. Mascini, I. Palchetti & S. Tombelli, "Nucleic Acid and Peptide Aptamers: Fundamentals and Bioanalytical Aspects," Angew. Chem. Int. Ed., vol. 50, pp. 2 – 19, 2011.

How to Cite this Article:

Akter, M., Parvez, M., Haque, E., Ferdous, H. & Matin, A. (2020). Fabrication of Carbon Nanotube (CNT) by Chemical Vapor Deposition and Investigate the Second Harmonic Response from CNT/Peptide and Si/SiO_2/Peptide Interfaces. International Journal of Science and Engineering Investigations (IJSEI), 9(101), 39-45. http://www.ijsei.com/papers/ijsei-910120-07.pdf